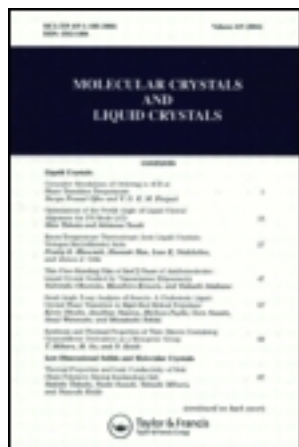


This article was downloaded by: [University of Haifa Library]

On: 14 August 2012, At: 09:09

Publisher: Taylor & Francis

Informa Ltd Registered in England and Wales Registered Number: 1072954 Registered office: Mortimer House, 37-41 Mortimer Street, London W1T 3JH, UK



## Molecular Crystals and Liquid Crystals

Publication details, including instructions for authors and subscription information:

<http://www.tandfonline.com/loi/gmcl20>

### Telecommunications Applications of LCOS Devices

W. A. Crossland<sup>a</sup>, T. D. Wilkinson<sup>b</sup>, I. G. Manolis<sup>b</sup>, M. M. Redmond<sup>b</sup> & A. B. Davey<sup>b</sup>

<sup>a</sup> Engineering Dept., Cambridge University, Trumpington St, Cambridge, CB2 1PZ E-mail:

<sup>b</sup> Engineering Dept., Cambridge University, Trumpington St, Cambridge, CB2 1PZ

Version of record first published: 18 Oct 2010

To cite this article: W. A. Crossland, T. D. Wilkinson, I. G. Manolis, M. M. Redmond & A. B. Davey (2002): Telecommunications Applications of LCOS Devices, *Molecular Crystals and Liquid Crystals*, 375:1, 1-13

To link to this article: <http://dx.doi.org/10.1080/10587250210552>

PLEASE SCROLL DOWN FOR ARTICLE

Full terms and conditions of use: <http://www.tandfonline.com/page/terms-and-conditions>

This article may be used for research, teaching, and private study purposes. Any substantial or systematic reproduction, redistribution, reselling, loan, sub-licensing, systematic supply, or distribution in any form to anyone is expressly forbidden.

The publisher does not give any warranty express or implied or make any representation that the contents will be complete or accurate or up to date. The accuracy of any instructions, formulae, and drug doses should be independently verified with primary sources. The publisher shall not be liable for any loss, actions, claims, proceedings, demand, or costs or damages whatsoever or howsoever caused arising directly or indirectly in connection with or arising out of the use of this material.



## Telecommunications Applications of LCOS Devices

W. A. CROSSLAND, T. D. WILKINSON, I. G. MANOLIS,  
M. M. REDMOND and A. B. DAVEY

*Cambridge University Engineering Dept., Trumpington St,  
Cambridge CB2 1PZ, wac@eng.cam.ac.uk*

### INTRODUCTION.

Liquid crystal liquid crystal over silicon (LCOS) devices can address large arrays of pixels at very high frame rates. They can also allow the phase of the light to be modulated in a manner that is independent of the state of polarisation of the incoming light. The optical versatility of the liquid crystal can now be matched by the electronic versatility of CMOS (complimentary metal oxide semiconductor) silicon backplanes as developments in very small feature sizes (sub micron) allows more and more complex electronic structures to be integrated into the device. In order to illustrate this, we briefly review a future application of this technology in the area of optical switching for telecommunications networks.

### INTELLIGENT CMOS BACKPLANES.

Recent innovations in deep sub-micron silicon technology combined with the explosion of the microdisplays market have greatly expanded the potential of next generation microdisplays. New 0.25 and 0.18 $\mu$ m processes have opened up the possibility of designing complex circuitry at each individual pixel and the development of planarisation based metal mirror processes means that the circuitry can be set beneath an optical quality pixel. Sub-pixel circuitry will not only revolutionise addressing techniques, it can also be used to create intelligent pixel devices allowing complex processing at the individual pixel level<sup>1,2</sup>. Intelligent pixels can be used in devices, which are not microdisplays, but are used to modulate the phase of the light rather than the intensity. There are a variety of applications for such spatial light modulators (SLMs) including telecommunications, as outlined in this paper as well as optical pattern recognition or correlators. Intelligence in the SLM silicon backplane can also be included, much like the wavelet compression system described for multimedia communications applications, exploiting the sub-micron silicon

VLSI processes and optical quality top layer planarisation and metallisation. An example of a possible intelligent telecomms LCOS SLM could be designed for an optically transparent switch. A critical issue in such an optical switch is the need for the optical path to be set and then left undisturbed ( $<0.1\text{dB}$  ripple) for long periods of time (possibly days, months or even years). This makes DC balancing the FLC material difficult as the traditional inverting frame technique would produce a glitch as all of the pixels were inverted. The solution to this problem is to use the shift invariance property of a hologram in order to balance the FLC. This technique is often referred to as scrolling the hologram, as a shift in the position of a hologram does not effect the intensity of its Fourier replay field. Hence, if we gradually shift the hologram in small increments, DC balancing can be achieved with only a small ripple in the optical connection power. A schematic example of scrolling a hologram pattern is shown in Figure 1. After multiple scrolling passes, each pixel has been in each state for equal amounts of time.



Figure 1. Example of a scrolled holographic pattern.

The scrolling scheme used to DC balance the FLC material can be implemented on the actual backplane of the LCOS SLM as it is just a series of interconnections between pixels where pixel data is transferred from one pixel to the next over the scrolled region. All that is required at each pixel is two single bit memory elements and a series of transfer gates that interconnect the pixels in the scrolling region. The act of transferring data between pixels is done using a state machine outside the area of the pixel array. In its simplest form, the state machine is just a sequence generator.

The key issue in using LCOS devices in telecomms applications is the performance of the FLC materials themselves, as this application is quite different compared to the traditional displays materials requirements. There are several ways in which the telecomms devices have to be optimised: The operating wavelength is 1550nm, hence the liquid crystal cell gap must be thicker to make the device a half wave plate in reflection. The pixel pitch must also be small (with low deadspace) to increase the steering angle and crosstalk. New FLC materials must also be used in the device to give the desired FLC tilt angle as close to  $45^\circ$  as possible. The current generation optical switches that are being designed at the moment will take microdisplay technology even further as they will use multi-level (grayscale) phase modulation, as this greatly improves the switch performance. Such LCOS devices can be made from customised grayscale microdisplay backplanes, with new liquid crystal

materials and electro-optical effects. Clearly very large arrays of small pixels can now be incorporated into LCOS switching devices. The limits are no longer defined by our ability to define and electronically drive the pixels, but by the liquid crystals. We will argue below that for scalable cross-connect switches their are advantages in using multi-level phase devices based on nematic liquid crystals. The same will be true for these devices

### OPTICALLY TRANSPARENT CIRCUIT SWITCHES.

Optically transparent switching will become a vital part of the modern vision of telecommunications networks. Integral to this is an optically transparent switch that is polarisation insensitive<sup>3,19</sup> and capable of low loss and low crosstalk<sup>4</sup>. A recent project has demonstrated the feasibility of an all-optical switch based on holographic beam steering using a ferroelectric liquid crystal (FLC) spatial light modulator (SLM)<sup>4</sup>. This project demonstrated that for low loss switching, a high tilt angle ( $\theta$  approaching  $45^\circ$ ) FLC material has to be used in the SLM. For this reason, a prototype 3x3 optical switch was built using a transmissive glass SLM containing the commercially available FLC material CS2005<sup>5</sup> which possesses a tilt angle of  $43^\circ$ . The transmissive SLM was designed as a 320x1 pixels glass SLM with  $20\mu\text{m}$  pitch pixels and  $2\mu\text{m}$  pixel deadspace<sup>6</sup>. The layout of the Indium Tin Oxide (ITO) tracks on the glass substrate is shown in Figure 2(a). The SLM was fabricated using standard class 100 cleanroom facilities to make a glass on glass 1D SLM. The  $20\mu\text{m}$  pixels were interdigitated (odd pixels at the top and even pixels at the bottom) and then fanned out to a  $180\mu\text{m}$  pitch 160 way connector at each edge of the glass. The glass cell was then connected to the driver circuitry via a 160 way flexi-cable bonded directly to the glass surface.

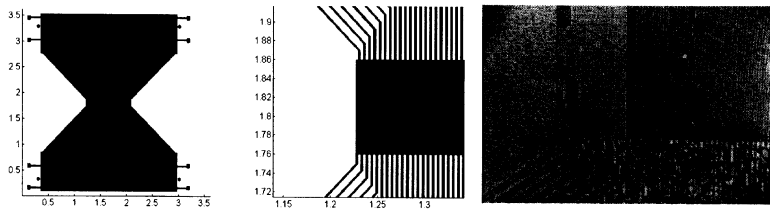


Figure 2: a) ITO on glass track layout of the pixels on the 320x1 SLM. b) Microscope image showing aligned area in the top right of the image.

The 3x3 switch demonstration was designed to operate at the telecommunications wavelength of  $1550\text{nm}$ . At this wavelength the birefringence ( $\Delta n$ ) of CS2005 is approximately 0.12. This implies a half wave cell thickness for transmissive modulation of  $6.3\mu\text{m}$  (or  $3.15\mu\text{m}$  for a reflective device). A pair of glass SLMs were made using rubbed nylon

alignment with a cell thickness measured at  $6.4\mu\text{m}$  and the LC subsequently aligned using a high voltage ( $10\text{ V}/\mu\text{m}$ ) at a frequency of  $1.8\text{ kHz}$  with a very small dc offset (10s of mV), just below the  $\text{Sc}^*\text{-N}^*$  phase transition. A region of the SLM pixels can be seen in Figure 2(b), showing the interdigitated ITO addressing and the alignment of the high-tilt FLC material. The region in the top left of Figure 2(b) is the active area of the SLM, where the pixels are side by side. Small areas of incorrect alignment are present near the edge of the array, and strong diagonal texturing is present, but alignment is very good compared to areas outside the array.

The liquid crystal properties of CS2005 were measured to determine the appropriate applied field and frequency characteristics for optimum operation, and the expected performance with increased temperature. The FLC properties of high tilt angle liquid crystalline materials, which lack Sa phases, are quite distinct from those manufactured for displays, and suffer from a lack of development. In particular the switching voltages required to achieve acceptable response times are typically higher, bistable operation is not straightforward and heat/field treatment is required to select a uniform layer orientation, ensuring adequate material alignment. However the theoretical efficiency of the device using high tilt FLC is not as sensitive to temperature over a large range (10's of degrees C) as one using a standard FLC would be, and higher diffraction efficiencies can be reached.

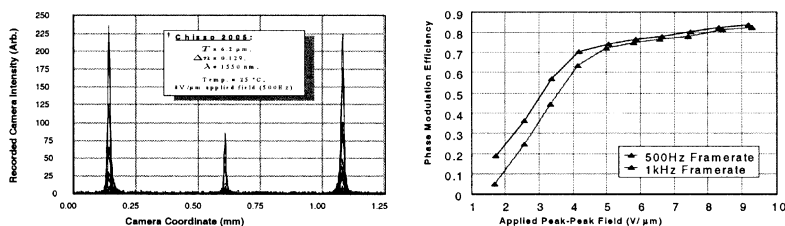


Figure 3(a & b). Diffracted orders of a cell driven at  $50\text{Vp-p}$  with a grating pattern

The aligned transmissive FLC SLM was tested in a polarisor-less 4f system at  $1550\text{nm}$ , imaged onto a CCD camera to test the diffraction performance. The results of this can be seen in Figure 3(a), where the diffraction peaks are shown at a drive voltage of  $50\text{Vp-p}$  ( $8\text{V}/\mu\text{m}$  at  $500\text{ Hz}$ ). Figure 4(b) shows a plot of the diffraction efficiency (normalised to an ideal of  $41\%$ ) of the hologram versus drive voltage. As the voltage increases, the tilt angle of the FLC material increases and the diffraction efficiency approaches the theoretical maximum of  $41\%$  for a single pixel binary grating. The final measured diffraction efficiency was  $35\%$ . The difference from the theoretical maximum of  $41\%$  was mostly due to the residual zero order that can be seen in

Figure 3(a). This may partly be due to the thickness of the cell not being exactly matched for half wave operation.

A  $N \times N$  channel holographic switch can be built using a single SLM, however, the scalability and performance is limited by the fan in to the output fibres. The routing of the light through large angles limits the number of ports that can be routed to, especially when using single mode structures at the output of the optical switch. A well-known solution to this problem is to build a holographic switch using two holograms as shown in Figure 4. This has the effect of improving the switch performance by reversing the deflection of the first hologram, with the opposite deflection angle at the second SLM. There is, however a fixed penalty in doing this, as the loss through the hologram is now doubled. This is particularly severe when using binary phase holograms, as the insertion loss is immediately increased from 4dB to 8dB through the 2 holograms.

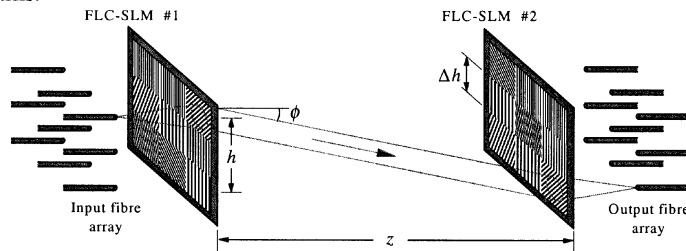


Figure 4. Two hologram optical switch architecture.

The architecture in Figure 4 is for a switch made from two-dimensional input and output arrays of optical fibres and hence will require a pair of two-dimensional SLMs. This is very impractical to demonstrate, as two-dimensional SLMs require complex addressing electronics and are ideally suited to silicon backplane reflective topologies. For this reason, the first demonstration of this architecture was done with a pair of one-dimensional SLMs. This meant that the single mode fibre arrays used in the ROSES switch could be used to implement the switch demonstrator. The one-dimensional architecture is shown in Figure 5.

The  $3 \times 3$  switch was built as a bench system, using catalogue lens components, which resulted in a switch that was over one metre long. This length could be greatly reduced, with both custom optics and reflective silicon backplane SLMs. The two SLMs were run without polarisers and at maximum tilt angle. The measured loss through the switch was 19.5dB (worst value) and the crosstalk was not able to be measured due to the limit of the photodetector (limit value -36dB). These results were originally met with pessimism, however a it was realised that the majority of the loss was due to non-optimal

ITO used on the transmissive SLMs. At 1550nm, the loss through the ITO was measured at  $-4\text{dB}$  per glass surface. In this switch there were 4 glass surfaces which means  $10\text{dB}$  of the loss was due to the ITO. Allowing a further  $8\text{dB}$  of loss due to the symmetry of the holographic replay from a binary phase hologram (two per channel) means that the actual loss due to the optics and fan-in was around  $0.5\text{-}1\text{dB}$ . This provides a very optimistic forecast for future switches with optimised SLMs at 1550nm. The loss in the ITO can be reduced to below  $1\text{dB}$  by thinning it. These results taken so far show that an efficient  $N \times N$  optical switch can be built using the two-hologram architecture. The results show that the CS2005 or a similar high tilt FLC material is well suited to efficient polarisation insensitive binary phase modulation. There are still issues to be addressed in terms of drive voltage and switching speed, however we have demonstrated a similar material with a lower switching angle, operating on a silicon backplane.

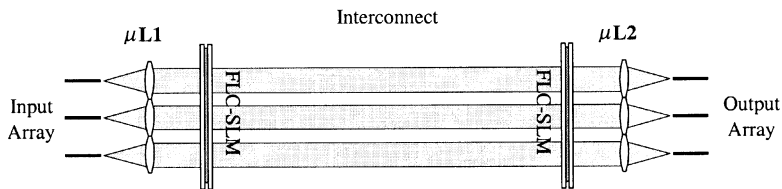


Figure 5. One-dimensional architecture of the two hologram  $3 \times 3$  switch demonstrator. (Optics in the centre has been omitted for simplicity)

The results from this work show that diffraction based liquid crystal optical switches can be made with suitable performance in terms of loss, crosstalk and polarisation dependence. The switches built so far have had small numbers of ports, however we have shown that the two hologram switch architecture can be used to overcome fan-in loss, which means that the switch is scalable to large port numbers. More importantly, the optical performance of the switch in terms of loss and crosstalk does not scale with the number of ports, hence if a  $3 \times 3$  switch can be made with  $8\text{dB}$  insertion loss, then it should be possible to make a  $128 \times 128$  port switch with an insertion loss less than  $10\text{dB}$ . This loss can be reduced by going to multi-level phase modulation in the liquid crystal SLM. Two hologram switches of with multi-level phase SLMs could have a significantly lower insertion loss<sup>18</sup> and beam selection by two holograms could greatly reduce the crosstalk to values below  $-40\text{dB}$ .

### MULTI-LEVEL PHASE MODULATION WITH NEMATICS.

There are two basic drawbacks when using FLCs in switch architectures. The first has to do with the addressing of the material itself. Although addressing schemes do exist for FLCs, they are all well adapted to display applications

and will fail in the case of optical transparent switching, mainly due to their associated optical flickering. The design of new addressing schemes is not always trivial and becomes problematic especially in cases where true bistability on the response of the material is not readily obtainable<sup>7</sup>. One solution to this problem is to use the shift invariance property of the hologram to DC-balance the material. This technique is often referred to as scrolling the hologram as a small shift in the position of the hologram does not affect the intensity of its Fourier replay. Hence, if we shift the hologram in small increments, DC balancing can be achieved with only a small ripple in the optical connection power. This technique is very well suited to intelligent pixel architectures as it can be very easily incorporated in the functionality of the circuitry embedded in each pixel, as shown in Figure 1.

More importantly, when using FLCs in switch architectures, the 4 dB loss associated with the binary phase nature of the FLC is intrinsic to the switch per hologram pass and cannot be reduced. The accumulated loss will be even higher if the deadspace between the pixels is taken under consideration. In a two-hologram configuration this will result to an insertion loss component of about -10 dB, which for some switching applications could be limiting. Additionally, symmetrical diffraction orders of a binary hologram can cause crosstalk problems in the switch and special care needs to be taken while designing binary patterns. Multi-level holograms can help to alleviate this problem as they can be designed to steer the light with very high efficiency and therefore to drastically improve the insertion loss and crosstalk figures of the switch. Having solved the scalability issues of a holographic switch by exploiting the fan-out/fan-in properties of a double hologram configuration, clearly, multi-level phase encoding is the next step.

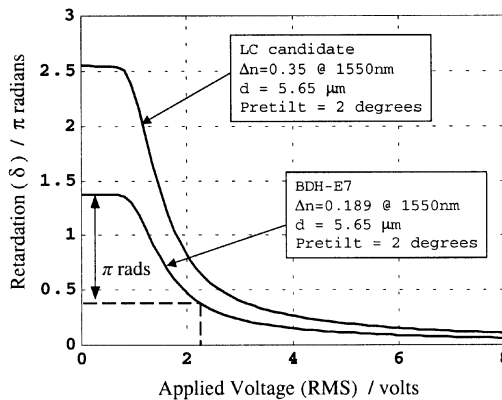


Figure 6 – Simulated phase modulation performance of nematic liquid crystal cells.



Nematic liquid crystal (NLC) materials offer a solution to the above problems associated with the employment of FLC in switch fabrics and undoubtedly are the candidates for the next generation of optical switches. Nematics in twisted, planar or homeotropic configurations can deliver electrically controlled continuous or multi-level phase modulation<sup>8</sup>, and have been used in the past to record phase-only holograms with the help of conventional liquid crystal display devices<sup>9,10</sup>. The simulated phase performance of a planar nematic cell filled with the nematic material BDH-E7 and at a wavelength of 1550 nm is shown in Figure 6. The thickness of the film has been taken to be 5.6  $\mu\text{m}$  and a small pretilt has been assumed on both glass surfaces. Continuous phase modulation of  $\pi$  radians is obtained for the first 2.25 volts of the applied voltage. The limited overall phase excursion is due to the reduced birefringence (0.189)<sup>11</sup> of the material at the operation wavelength and can be greatly improved, as shown by the second curve in Fig. 6, by using a different material with enhanced birefringence at 1550 nm.

In addition to their capacity for multiple-level phase modulation, nematics, being RMS responding materials, can be addressed in a much more straightforward way than ferroelectrics. There is no particular need to DC-balance the material using special techniques as this is already incorporated in the AC driving waveform that is used to produce the desired switching effect. Accordingly, well-tested addressing schemes originally developed for display applications can be readily used as they are in holographic switches without affecting their performance.

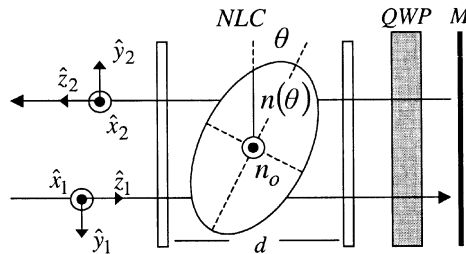


Figure 7 – Polarisation insensitive configuration with a nematic device. The QWP has been aligned with its axis at  $45^\circ$  to the optical axis of the NLC layer.

The potential of nematic liquid crystals for the implementation of optical interconnections through holographic beam steering has been reported already<sup>12,13</sup>. All these proposed architectures, however, suffer from polarisation sensitivity and therefore they cannot directly be used. Circuit switches suitable for optical networks have no polarisation control hence polarisation insensitivity is vital. A way around this problem is to use an

arrangement, which allows nematics to modulate the phase of the light independently from their polarisation state. The arrangement incorporates a quarter-wave plate (QWP) and a mirror in a reflective configuration and is shown in Figure 7. The QWP has been aligned with its extraordinary axis on the  $xy$ -plane at an angle of  $45^\circ$  to the optical axis of the LC film.

The underlying principle of the proposed technique has been reported in the literature already; in the first case for clock distribution among electronic chips<sup>14</sup> and in the second case for wavefront correction<sup>15</sup>. Shutters for unpolarised light<sup>16</sup> and a variable, polarisation-insensitive liquid crystal (LC) phase retarder<sup>17</sup> have been also demonstrated using the same concept. Here we use the principle to generate reconfigurable pixellated multilevel phase holograms to steer the near infrared light from single mode optical fibres such that the power in the routed beam is independent of the state of polarisation of the incoming light.

On the first pass through the device, polarisation components along the  $y$ -axis experience the extraordinary refractive index  $n(\theta)$  of the nematic material, while components parallel to the  $x$ -axis only the ordinary refractive index  $n_o$ . The combination of the QWP and the mirror acts as a  $90^\circ$  polarisation-rotator for the two orthogonal components thus mutually exchanging their polarisation states. On the second pass from the device, components, which were previously polarised along the  $x$ -axis are now parallel to the  $y$ -axis and therefore experience a refractive index of  $n(\theta)$  while components previously polarised along the  $y$ -axis, are now parallel to the  $x$ -axis and they only experience the ordinary refractive index of the material. In that way, both orthogonal polarizations are subject to the same overall retardation of  $d = k_0 d(n(\theta) + n_o)$  where  $k_0$  is the wavenumber in the free space and  $d$  is the thickness of the LC layer.

More specifically, in the general case of a material with non-negligible absorption anisotropy, the Jones matrix representation for the LC film in the given coordinate system for the first pass through the device will be:

$$N_1 = \begin{bmatrix} \exp(-da_o - jk_0dn_o) & 0 \\ 0 & \exp(-da(\theta) - jk_0dn(\theta)) \end{bmatrix}$$

Where  $a_o$  and  $a(\theta)$  are the absorption coefficients of the film along the  $x$ - and  $y$ - axis respectively. The absorption of a typical nematic material in the infrared region is normally very small, however, for materials optimised to deliver increased phase modulation around 1550 nm this might not be the case. The Jones matrix for the QWP in the given coordinate system, ( $Q_1$ ), can be easily calculated. Similar expressions will hold for the second pass through the QWP ( $Q_2$ ) and LC layer ( $N_2$ ). Assuming a random state of polarisation for the input light, represented by the vector  $\mathbf{E}_{IN} = [\rho_x, \rho_y \exp(jr)]$ , the output polarization will be given by  $\mathbf{E}_{OUT} = N_2 Q_2 M Q_1 N_1 \mathbf{E}_{IN}$ , where  $M$  is the matrix

representing the effect of the mirror on the propagating light. This is equivalent to exchanging from the  $x_1y_1z_1$  to the  $x_2y_2z_2$  coordinate system in Figure 7. Performing the calculations we obtain:

$$\mathbf{E}_{\text{OUT}} = \begin{bmatrix} \rho_y \cdot \exp[-d(a_o + a(\theta))] \cdot \exp[-j(dk_0(n_o + n(\theta)) - r - \pi)] \\ \rho_x \cdot \exp[-d(a_o + a(\theta))] \cdot \exp[-j(dk_0(n_o + n(\theta)))] \end{bmatrix}$$

Hence, for any tilt angle  $\theta$ , both polarization components receive the same amount of phase retardation and amplitude attenuation. Therefore a spatial arrangement of switching states across the  $xy$  plane ( $\theta = \theta(x, y)$ ), by means of a spatial light modulator (SLM) for example, will produce an identical holographic pattern for both orthogonal polarization modes. This is equivalent to obtaining polarization insensitivity in the operation of a holographic switch. The validity of this new approach was verified experimentally by measuring the power of the two main diffraction orders (+1 and -1) from a collimated beam of light (1550nm) incident on a nematic one-dimensional SLM arranged with a QWP and a mirror as in figure 7. The experimental setup used is shown in Figure 8. The two diffraction spots were collected on the photo-detector D, using a mirror-slide carefully positioned on the plane A. A simple pattern was displayed on the 100 $\mu\text{m}$  pixel-pitch glass SLM by keeping grounded all odd electrodes together with the front electrode of the SLM and applying a sinusoidal driving waveform of 1 kHz on all even electrodes. The SLM used had a thickness of  $5.56 \pm 0.01 \mu\text{m}$  and was filled with the LC E7.

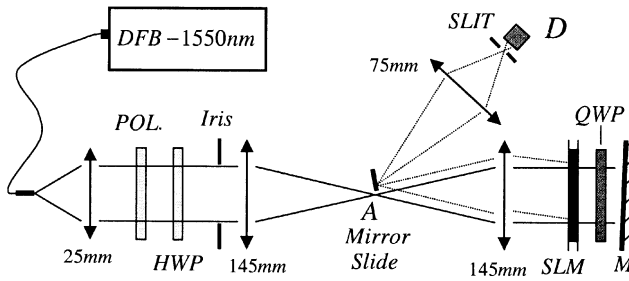


Figure 8 - Experimental confirmation of multi-level polarisation insensitive phase modulation with a nematic device (E7)

Polarisation insensitivity was confirmed by monitoring the power of the two spots while rotating the input polarisation utilising a HWP combined with polariser in the path of the beam. These results (Figure 9(a)) showed that the power variation of the diffracted spots was indeed very minor (less than 0.5dB) with varying input polarisation.

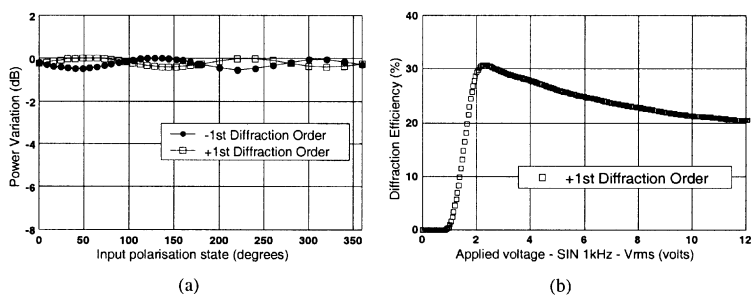


Figure 9 – Diffraction efficiency of the nematic device as a function of (a) input polarisation and (b) applied voltage

Multi-level phase operation was confirmed by monitoring the diffraction efficiency of the SLM as a function of the applied voltage on its electrodes. By adjusting the applied voltage we were able to continuously change the corresponding phase step among alternating pixels thus altering the efficiency of the hologram. The results are shown in Figure 9(b) for the +1 order. An identical curve was obtained for the -1 order. The efficiency increases as the phase step between subsequent pixels approaches the optimum value of  $\pi$  radians. The maximum measured diffraction efficiency was 32 %, which is in close agreement with the theoretically predicted value of 33 % for a binary phase grating recorded on a device with a 10% pixel deadspace<sup>18</sup>. As shown in the same graph the voltage level where the optimum performance is obtained is approximately 2.2 volts (RMS), which is in good agreement with the simulated phase modulation performance curve of a planar E7 cell given in Figure 6.

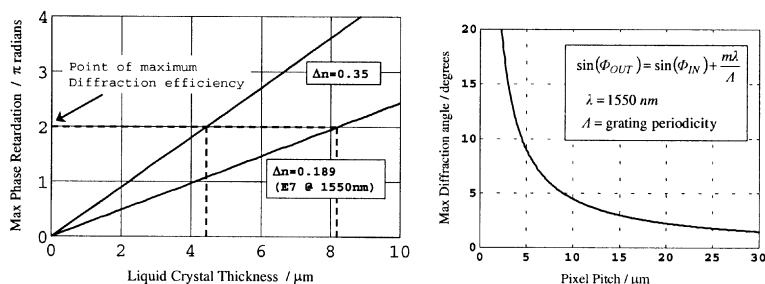


Figure 5 a) Increased birefringence on the LC film thickness required for optimum phase operation b) Diffraction angle as a function of pixel pitch

There is always a trade-off between achievable phase modulation range, LC film thickness and material birefringence at the operation wavelength. Multi-level phase holograms with a phase excursion of  $2\pi$  radians are essential for making low-loss optical switches. A diffraction efficiency of  $>77\%$  (10% deadspace is assumed) is theoretically achievable<sup>18</sup> if eight phase levels were used to write the hologram instead of just two, and further improvements should be expected by using even more phase levels. However, a phase excursion of  $2\pi$  radians implies thicker devices, which in turn would mean slow switching speeds for the available voltages on the chip. In this case, using a material with a high birefringence at the operational wavelength (1550nm) would be of significant advantage. This is clearly shown in Figure 10(a) where the required thickness for optimum operation of a device filled with the LC E7 is compared with the case a LC with increased birefringence at 1550nm ( $\Delta n=0.35$ ).

Finally, in our experiment a maximum diffraction angle of approximately  $0.44^\circ$  was obtained by the  $100\mu\text{m}$  pixel pitch ( $200\mu\text{m}$  grating periodicity). A pixel pitch of  $10\mu\text{m}$  (typical of that in liquid crystal over silicon microdisplay devices) would give a maximum diffraction angle of  $4.4^\circ$  (Figure 10(b)) and a capability to address more switch ports. Available silicon backplane technology allows very much smaller pixels ( $<10\mu\text{m}$ ) to be addressed in very large arrays. The limits of pixel size and therefore diffraction angle are set by the liquid crystal properties and several aspects of this limit remains to be explained and understood.

## REFERENCES

- 1 A. M. Rassau, K. Eshraghian, H. Cheung, S. W. Lachowicz, T. C. B. Yu, W. A. Crossland and T. D. Wilkinson, "Wavelet transform algorithms for smart pixel opto-VLSI implementation", Int. Conf. on Computational Engineering and Systems Applications, Tunisia, April 1998.
- 2 A. M. Rassau, S. Chae, K. Eshraghian, "Simple binary wavelet filters for efficient VLSI implementation", *Electronics Letters*, 35(7), 1999, pp555-557
- 3 S.T. Warr and R.J. Mears, "Polarisation insensitive operation of ferroelectric liquid crystal devices", *Electronics Letters*, 31, 714-716, 1995
- 4 W. A. Crossland, I. G. Manolis, M. M. Redmond, K. L. Tan, T. D. Wilkinson, M. J. Holmes, T. R. Parker, H. H. Chu, J. Croucher, V. A. Handerek, S. T. Warr, B. Robertson, I. G. Bonas, R. Franklin, C. Stace, H. J. White, R. A. Woolley, G. Henshall, "Holographic Optical Switching: The 'ROSES' Demonstrator" *J. of Lightwave Tech*, 18(12), 2000, p1845
- 5 CS2005 material from the Chisso Corporation, Japan.
- 6 T. D. Wilkinson, M. M. Redmond, S. T. Warr, B. Robertson, and W. A. C. Crossland, "High tilt angle ferroelectric liquid crystal spatial light

- modulator for optical interconnects”, *IEE Electronics and Communications Meeting, ‘Microdisplay and Smart Pixel Technologies’*, London, March, 2000
7. I.G. Manolis, M.M. Redmond, W.A. Crossland, A.B. Davey, and T.D. Wilkinson, “Control of the electro-optic bistability of some ferroelectric liquid crystals useful for binary phase optical modulators”, *Mol. Cryst. Liq. Cryst.* 351: 305-314, (2000).
  8. N. Konforti, E. Marom, and S.-T. Wu, “Phase-only modulation with twisted nematic liquid-crystal spatial light modulators”, *Optics Letters*, 13(3): 251-253, 1988.
  9. F. Mok, J. Diep, H.-K. Liu, and D. Psaltis, “Real-time computer generated hologram by means of liquid-crystal television spatial light modulator”, *Optics Letters*, 11(11): 748-750, 1986.
  10. T.H. Barnes, T. Eiju, K. Matsuda, and N. Ooyama, “Phase-only modulation using twisted nematic liquid crystal television”, *Applied Optics*, 28(22): 4845-4852, 1989.
  11. Measurements made by M. Warengam and M. Redmond at Univerisite d’Artois, Lens
  12. H. Yamazaki and M. Yamaguchi, “4 x 4 free-space optical switching using real-time binary phase-only holograms generated by a liquid-crystal display”, *Optics Letters*, 16(18): 1415-1417, 1991.
  13. H. Ichikawa, T.H. Barnes, M.R. Taghizadeh, J. Turunen, T. Eiju, and K. Matsuda, “Dynamic space-variant optical interconnections using liquid crystal spatial light modulators”, *Optics Communications*, vol. 93, pp.145-150, 1992.
  14. E. Marom and N. Konforti, “Dynamic optical interconnections”, *Optics Letters*, 12(7): 539-541, July 1987.
  15. G.D. Love, “Liquid-crystal phase modulator for unpolarised light”, *Applied Optics*, 32(13): 2222-2223, 1993.
  16. D. Ulrich, C. Tombling, J. Slack, P. Bonnett, B. Henley, M. Robinson, and D. Anderson, “A diffraction based polarisation independent lightvalve”, presented at the IEE Seminar on Microdisplay and Smart Pixel Technologies, IEE. 2000, pp.8/1-6. London, UK, 17 March 2000.
  17. Y. Morita, J.E. Stockley, K.M. Johnson, E. Hanelt, and F. Sandmeyer, “Active liquid crystal devices incorporating liquid crystal thin film waveplates”, *Jpn. J. Appl. Phys. Part 1*, 38 (1A): 95-100, (1999).
  18. K.L. Tan, S.T. Warr, I.G. Manolis, T.D. Wilkinson, M.R. Redmond, W.A. Crossland, R.J. Mears, and B. Robertson, “Dynamic holography for optical interconnections. II. Routing holograms with predictable location and intensity of each diffraction order,” *J. Opt. Soc. Am. A*. 18 (1), 205-215 (2001).
  19. M.J. O’Callaghan and M.A. Handschy, “Diffractive ferroelectric liquid-crystal shutters for unpolarized light”, *Opt. Lett.*, 16 (10): 770-772, (1991).